

Reversible resistance switching in $\text{La}_{0.225}\text{Pr}_{0.4}\text{Ca}_{0.375}\text{MnO}_3$: The Joule-heat-assisted phase transition

Z. B. Yan, K. F. Wang, S. Z. Li, S. J. Luo, and J.-M. Liu^{a)}

Nanjing National Laboratory of Microstructures, Nanjing University, Nanjing 210093, People's Republic of China and International Center for Materials Physics, Chinese Academy of Sciences, Shenyang 110016, People's Republic of China

(Received 31 May 2009; accepted 10 September 2009; published online 6 October 2009)

The reversible resistance switching (RS) controlled by current pulse pairs, accompanied with overshooting relaxation, is observed in bulk $\text{La}_{0.225}\text{Pr}_{0.4}\text{Ca}_{0.375}\text{MnO}_3$. We demonstrate that the reversible RS effect is not the result of current-induced intrinsic transition of charge-insulator (COI) into ferromagnetic metal (FMM) phase, but the outcome of Joule-heat-assisted transition between the FMM and COI phases. A local thermal-cycle assisted rearrange FMM phase in the COI matrix is controllable by a current pulse, opening a possibility memory applications. © 2009 American Institute of Physics. [doi:10.1063/1.324197]

Reversible resistance switching (RS), i.e., repeated switching between the high resistance state (HRS) and low resistance state (LRS), is attracting attention due to its potential applications in resistive random access memories.¹⁻³ The RS effect was already observed in many metal-insulator-metal systems, in which the insulator layer ranges from oxides to chalcogenides and even organics.^{1,2} This effect is believed to originate from formation and rupture of conductive filaments in insulator matrix or at the interface between the metal electrode and the insulator. It can be driven by many mechanisms such as amorphous-crystalline state transitions, electrochemical migration of oxygen, and order-disorder transitions of polarons at the metal-oxides interface.¹⁻⁴

The RS effect is also observable in some strongly electron correlated systems in which the interaction between charge, spin, and lattice degrees of freedom is expected to induce complicated phenomena.^{5,6} For example, the electronic phase separation in manganites, i.e., the coexistence of charge-ordered insulator (COI) phase and ferromagnetic metal (FMM) phase provides a new mechanism. A melting of the COI phase and/or enlargement of the FMM phase, driven by voltage/current, leads to the volatile or nonvolatile RS from the HRS to the LRS, i.e., colossal electroresistance (CER).^{7,8}

Although the mechanism of RS is still elusive. For example, the RS effect can be induced by Joule self-heating, which is usually associated with the Joule self-heating effect. In the $\text{La}_{5/8-y}\text{Pr}_y\text{Ca}_{3/8}\text{MnO}_3$ series exhibit the coexisting COI and FMM phases at nanometer or submicrometer scale and thus fascinating dynamic behaviors.^{8,12} In this work, we observe a reversible RS effect, accompanied by an overshooting relaxation, in $\text{La}_{0.225}\text{Pr}_{0.4}\text{Ca}_{0.375}\text{MnO}_3$ (LPCMO), which can be uniquely controlled by current pulse pair. The thermal-cycle experiment and resistance-current (R - I) characterization indicate that the RS effect in the present case is irrelevant to the intrinsic CER effect, but the outcome of FMM phase rearrangement in the COI matrix, with assistance of the Joule heating.

The polycrystalline standard solid-state resistivity measurement revealed no magnetoresistance (M) was measured using the four-probe configuration used [see Fig. 1]. The RS effect was observed in the sample, the size of which was $8.40 \text{ mm} \times 2.26 \text{ mm} \times 1.54 \text{ mm}$. The RS effect was measured using the four-probe method. The RS effect was observed in the sample, the size of which was $8.40 \text{ mm} \times 2.26 \text{ mm} \times 1.54 \text{ mm}$. The RS effect was measured using the four-probe method.

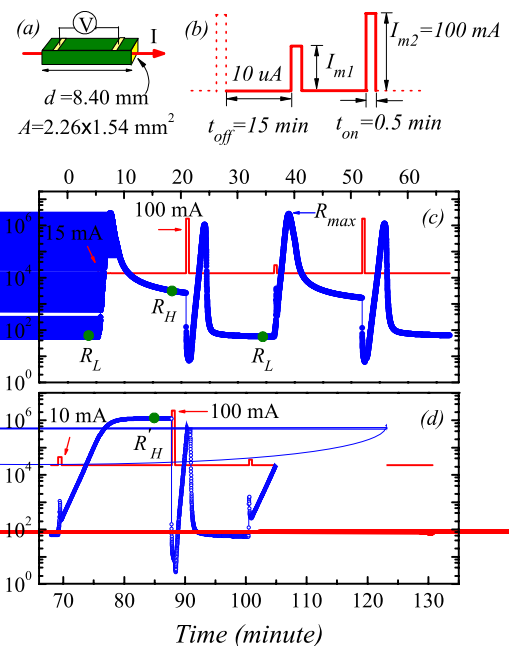


FIG. 1. (Color online) [(a) and (b)] Measuring configuration and the periodical current pulse-pair used for the RS measurement, respectively. [(c) and (d)] Time dependent resistance at $T = 10 \text{ K}$, with $I_{m1} = 15 \text{ mA}$ and 10 mA , respectively. Red curve: the current used for the measurement.

^{a)} Author to whom correspondence should be addressed. Electronic mail: liujm@nju.edu.cn.

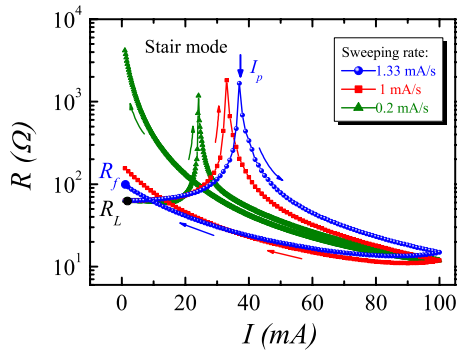


FIG. 2. (Color online) Resistance-current (R - I) characteristics at the LRS, measured in four-probe configuration by the current sweeping in the stair mode with the rate 1.33 mA/s (blue sphere), 1 mA/s (red square), and 0.2 mA/s (olive up-triangle), respectively.

temperature measurements were performed at a rate of 2 K/min.

First, looking at the RS effect, we measure R by cooling the sample from 300 K down to 10 K, by which a pristine LRS with $R=R_L \sim 60 \Omega$ can always be obtained. Then periodical electric current pulse-pairs with one pulse I_{m1} and the other pulse I_{m2} [Fig. 1(b)] are applied onto the sample. Here a persistent bias current of $10 \mu\text{A} \ll I_{m1}(I_{m2})$ is always applied in order to measure R after the pulse off. It is noted that all the pulses have the same width (pulse-on time) $t_{\text{on}} = 0.5 \text{ min}$. The interpulse interval (pulse-off time) $t_{\text{off}} = 15 \text{ min}$ is fixed. Typically, as $I_{m1} = 15 \text{ mA}$ and $I_{m2} = 100 \text{ mA}$, a reversible RS effect accompanied with an overshooting relaxation is observed, as shown in Fig. 1(c). After pulse I_{m1} , R relaxes via a sharp overshooting path, bringing the system from the LRS to the HRS with $R=R_H \sim 10^3 \Omega$, which is almost two orders of magnitude larger than R_L . Here, R_H is defined as the resistance at 13 min apart from I_{m1} where the relaxation becomes negligible, although its value may not be strictly defined. However, by subsequent pulse I_{m2} , R is switched back to the LRS, i.e., from R_H to R_L . This sequence illustrates how the reversible RS between the HRS and LRS proceeds.

The results also show that pulse I_{m1} has significant impact on R_H of the HRS but has not much on R_L of the LRS. In Fig. 1(d), as an example, choosing $I_{m1} = 10 \text{ mA}$ leads to another HRS with $R=R'_H \sim 10^6 \Omega$, which is almost three orders of magnitude larger than R_H at $I_{m1} = 15 \text{ mA}$. The HRS with $R=R'_H$ can persist for very long time until a subsequent pulse $I_{m2} = 100 \text{ mA}$ brings the system back to the LRS with $R=R_L$. This suggests that multiple memory states can be reached by choosing different pulse-pairs (I_{m1} , I_{m2}).

Surely, this RS effect is also sensitive to the pulse width. If one shortens t_{on} down to 6 ms from 30 s, retaining $I_{m1} = 15 \text{ mA}$ and $I_{m2} = 100 \text{ mA}$, no more nonvolatile RS effect can be observed. This allows us to argue that the assisting effect of the Joule heating rather than the intrinsic CER effect contributes to the nonvolatile RS effect.

For evaluating the Joule heating effect, we remeasure the R - I curves at the LRS in the four-probe configuration using the stair mode with various sweeping rates at 10 K. As shown in Fig. 2, when I is swept from 0 to 100 mA at a rate of 1.33 mA/s, R increases from R_L and reaches a steep peak at $I_p = 37 \text{ mA}$, after which R falls rapidly down. The variation of R is one order of magnitude or more. The subsequent

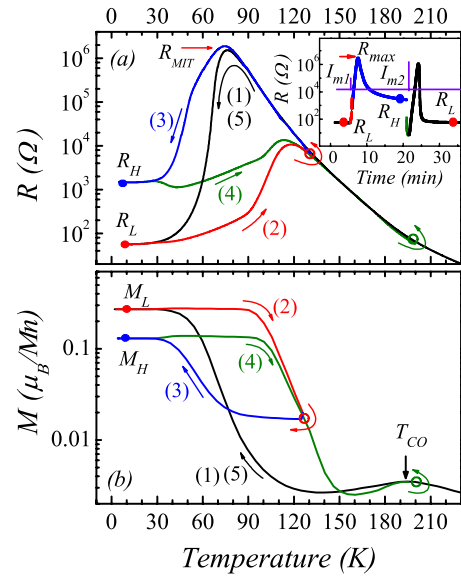


FIG. 3. (Color online) [(a) and (b)] Temperature dependent resistance $R(T)$ at $10 \mu\text{A}$ and magnetization $M(T)$ at 100 Oe, respectively, in the sequence from path (1) to (5), i.e., $T=300 \rightarrow 10 \rightarrow 130 \rightarrow 10 \rightarrow 200 \rightarrow 10$ (K). Inset: the local data of Fig. 1(c), redrawn with several colors assigned to the path (1), (2), (3), and (4), respectively. The violet line is the measuring current.

back-sweeping of I from 100 mA to 0, however, causes a continuous increase of R up to $R_f > R_L$. At the rate of 1.0 and 0.2 mA/s, the current I_p , corresponding to the peak of R , downshifts to 33 and 24 mA, respectively. The lower the sweeping rate, the larger the resistance R_f .

Unquestionably, the CER effect and the isothermal relaxations contribute to the experimental data. But they cannot explain the presence of the cuplike peak. Earlier investigations already observed the similar cuplike peak in R - I curve on LPCMO, and explained it by the Joule-heat-induced metal-to-insulator transition.^{11,13} During the current forth-sweeping at 10 K, the Joule-heat leads to the continuous increase of the local temperature, and R increases first due to the metallic behavior and then decreases after transitioning into the insulating state at I_p , displaying a cuplike peak in R - I curve. A lower sweeping rate implies the longer current persistent time and thus larger amount of Joule heat generated during the sweeping process, leading to a lower I_p and a higher R_f . The data shown in Fig. 2 clearly indicate that the Joule heating drives such a transition occurring at I_p and eventually causes $R_f > R_L$.

Now we come to illustrate a nonvolatile RS effect between the LRS and HRS under the assistance of thermal cycles. We perform two consecutive near-equilibrium thermal cycles in a sequence $T=300 \rightarrow 10 \rightarrow 130 \rightarrow 10 \rightarrow 200 \rightarrow 10$ K, with a bias dc current $10 \mu\text{A}$ and a magnetic field 100 Oe for measuring R and M , respectively, as shown from path (1) to (5) in Fig. 3. For cycle one, along path (1), the sample cooling from 300 K leads to a transition from the paramagnetic-insulating (PMI) state to the COI state at $T_{\text{CO}} \sim 190 \text{ K}$ and from the COI state to the FMM state at $T_{\text{MIT}} \sim 76 \text{ K}$, until the pristine LRS at $T=10 \text{ K}$. Starting from this LRS state, by warming the sample to $T=T_h=130 \text{ K}$ and re-cooling it back to $T=10 \text{ K}$, i.e., along paths (2) and (3) in sequence, the resistance is switched from R_L to R_H , while M decreases from M_L to M_H at $T=10 \text{ K}$. Cycle two, which is a thermal cycle between $T=10 \text{ K}$ and $T_h=200 \text{ K}$ via paths (4) and (5), can drive the system from the HRS to the LRS. In a

word, the above two thermal cycles allow a reversible RS between the HRS and LRS.

We performed the thermal-cycling experiments with T_h from 110 to 300 K. It was noted that when $T_h > T_{CO} \sim 190$ K, the cooling path from T_h to 10 K, like path (5), is coincident with path (1), indicating that the LRS is always reachable as long as the sample is cooled from $T_h > 190$ K.

It should be mentioned here that at $T < 30$ K the system actually enters a blocked (frozen) state in which the phase separation is blocked (frozen).¹² Hence, the HRS and LRS can be utilized in nonvolatile memory.

The RS effect between the LRS and HRS can be understood by the first-order phase transitions between the FMM and COI phases in LPCMO.¹⁴ It is indicated that given a T below the critical point T_c , the low- T FMM phase nucleates and grows from the supercooled COI matrix. For a thermal-cycle between 10 K and T_h ($T_h > T_c$), the low- T FMM phase is decomposed as heating to T_h and then is recrystallized as cooling to 10 K again. As the annealing conditions such as T_h and cooling rate are changed, the growth of low- T FMM phase will be significantly influenced, leading to the different phase-separated state at low temperature.^{14,15}

The reason why cooling from $T_h > T_{CO}$ (e.g., $T_h \sim 200$ K or even 300 K) ends up with the LRS is given below. As $T > T_{CO}$, there is only PMI phase and the R - T and M - T curves have no any hysteresis, indicating the history independence in this temperature region. So the cooling from $T_h > T_{CO}$ follows the same path [path (1)].

However, cooling from $T_h < T_{CO}$ leads to a lower FMM fraction and ends up with the HRS at 10 K. Beside, the different T_h ends up with different HRS. In this case, path (3), as an example, is outside the major loop consisting of path (1) and (2). It indicates the presence of an additional factor controlling the hysteretic behavior. In earlier studies, it was shown that the short-range and inhomogeneous strain plays an important role in the first-order magnetic phase transition of LPCMO.^{16–19} Accompanied by the COI-to-FMM phase transition, the interfacial elastic energy arises due to the coexistence of FMM and COI domains with distinct lattice mismatch and different surface/volume ratios.¹⁹ The increase of the interfacial elastic energy in turn raises the energy barrier and impedes the growth of FMM phase.^{16–18} With the thermal cycling within the FMM-COI coexistence temperature region (between 10 K and $\sim T_{CO}$, in the present case), the intertransition between FMM and COI phases may bring out additional FMM-COI interfacial regions that increase the interfacial elastic energy and complicate the free-energy landscape. This may be the major reason for favoring a smaller FMM fraction at lower T after the thermal cycles, giving rise to a larger resistivity.

As driven by the periodical current pulse-pairs, the local data of Fig. 1(c) is redrawn in the inset of Fig. 3, with several colors assigned to path (1), (2), (3), and (4), respectively. Due to the percolation-type transport of LPCMO, the Joule heating generated by the pulse I_{m1} (e.g., $I_{m1} = 15$ mA) arises the local T of the FMM filaments rapidly, and consequently destabilizes the FMM phase and drives its transition (decomposition) back to high- T COI state, featured with the filament rupture. Because of the insulating behavior of the ruptured filament at high T , subsequent removal of I_{m1} allows falling-

down of the local T and enhancement of R . Further decreasing of T below T_c enables growth of the isolated FMM domains from the COI matrix and leads to recapture of the FMM filaments, at which R begins to fall down, constituting an overshooting relaxation phenomena.

The removal of $I_{m1} = 10$ mA is a special situation, in which nonovershooting relaxation phenomena observed. After the removal of $I_{m1} = 10$ mA, the increase of FMM fraction may be not enough to link the ruptured filaments, leading to the persistence in the insulating state with much higher resistance at 10 K. This may be the reason why no overshooting relaxation is displayed in Fig. 1(d).

The process after the removal of pulse I_{m1} is similar with that of the path (3). When the local T eventually returns back to 10 K, the HRS instead of the LRS is reached due to a smaller FMM fraction nucleated. However, imposing pulse $I_{m2} = 100$ mA can raise the local T of the FMM filaments up to a value much higher than T_{CO} , causing a complete decomposition of the FMM phase and COI phase into PMI phase and finally disappearing the filaments and wiping out the history at high T . The subsequent cooling process after the removal of I_{m2} , similar with that of the path (1), leads to the LRS at 10 K eventually. The assistance of the two consecutive thermal cycles thus enables the reversible RS effect between the HRS and LRS.

This work was supported by the Natural Science Foundation of China (Grant Nos. 50601013 and 50832002), the National Key Projects for Basic Research of China (Grant Nos. 2006CB921802 and 2009CB623303), and the 111 Programme of MOE of China (Grant No. B07026).

¹R. Waser and M. Aono, *Nature Mater.* **6**, 833 (2007).

²A. Sawa, *Mater. Today* **11**, 28 (2008).

³M. Wuttig and N. Yamada, *Nature Mater.* **6**, 824 (2007).

⁴C. Jooss, J. Hoffmann, J. Fladerer, M. Ehrhardt, T. Beetz, L. Wu, and Y. Zhu, *Phys. Rev. B* **77**, 132409 (2008).

⁵D. S. Kim, Y. H. Kim, C. E. Lee, and Y. T. Kim, *Phys. Rev. B* **74**, 174430 (2006).

⁶M. Quintero, P. Levy, A. G. Leyva, and M. J. Rozenberg, *Phys. Rev. Lett.* **98**, 116601 (2007).

⁷A. Asamitsu, Y. Tomioka, H. Kuwahara, and Y. Tokura, *Nature (London)* **388**, 50 (1997).

⁸H. Sakai and Y. Tokura, *Appl. Phys. Lett.* **92**, 102514 (2008).

⁹H. Song, M. Tokunaga, S. Imamori, Y. Tokunaga, and T. Tamegai, *Phys. Rev. B* **74**, 052404 (2006).

¹⁰L. Zhang, C. Israel, A. Biswas, R. L. Greene, and A. de Lozanne, *Science* **298**, 805 (2002).

¹¹M. Tokunaga, Y. Tokunaga, and T. Tamegai, *Phys. Rev. Lett.* **93**, 037203 (2004).

¹²L. Ghivelder and F. Parisi, *Phys. Rev. B* **71**, 184425 (2005).

¹³A. Rebello and R. Mahendiran, *Appl. Phys. Lett.* **94**, 112107 (2009).

¹⁴K. Kumar, A. K. Pramanik, A. Banerjee, P. Chaddah, S. B. Boy, S. Park, C. L. Zhang, and S.-W. Cheong, *Phys. Rev. B* **73**, 184435 (2006).

¹⁵P. Chaddah, K. Kumar, and A. Banerjee, *Phys. Rev. B* **77**, 100402(R) (2008).

¹⁶P. A. Sharma, S. El-Khatib, I. Mihut, J. B. Betts, A. Migliori, S. B. Kim, S. Guha, and S.-W. Cheong, *Phys. Rev. B* **78**, 134205 (2008).

¹⁷R. Mahendiran, B. Raveau, M. Hervieu, C. Michel, and A. Maignan, *Phys. Rev. B* **64**, 064424 (2001).

¹⁸V. Markovich, I. Fita, R. Puzniak, C. Martin, A. Wisniewski, C. Yaicle, A. Maignan, and G. Gorodetsky, *Phys. Rev. B* **73**, 224423 (2006).

¹⁹J. Fan, B. Hong, Y. Ying, L. Ling, L. Pi, and Y. Zhang, *J. Phys. D: Appl. Phys.* **41**, 105013 (2008).